EARTH SURFACE PROCESSES AND LANDFORMS
Earth Surf. Process. Landforms **36,** 923–932 (2011)

Published online 16 December 2010 in Wiley Online Library
(wileyonlinelibrary.com) DOI: 10.1002/esp.2122

A simple model accounting for the uptake, transport, and deposition of wind-eroded mineral particles in the hyperarid coastal Atacama Desert of northern Chile

Stephane C. Alfaro,[1]* Valentina Flores-Aqueveque,[1,2] Gilles Foret,[1] Sandrine Caquineau,[3] Gabriel Vargas[2] and Jose A. Rutllant[4]
[1] LISA, UMR CNRS/INSU 7583, Université de Paris-Est, 61 av. du General de Gaulle, Créteil, France
[2] Departamento de Geología, Facultad de Ciencias Físicas y Matemáticas, Universidad de Chile, Plaza Ercilla 803, Santiago, Chile
[3] IPSL/LOCEAN, UMR 7159 – IRD-CNRS-UPMC-MNHM, Institut de Recherche pour le Développement, 32 av. Henri Varagnat, 93143, Bondy cedex, France
[4] Departamento de Geofísica, Facultad de Ciencias Físicas y Matemáticas, Universidad de Chile, Blanco Encalada 2002, Santiago, Chile

Received 31 March 2010; Revised 11 November 2010; Accepted 16 November 2010

*Correspondence to: S.C. Alfaro, LISA, UMR CNRS/INSU 7583, Université de Paris-Est, 61 av. du General de Gaulle, Créteil, France.
Email: alfaro@lisa.univ-paris12.fr

ESPL
Earth Surface Processes and Landforms

ABSTRACT: As previously observed in marine sediments collected downwind of African or South American continental sources, recent studies of sediment cores collected at the bottom of Mejillones Bay in north Chile (23°S) show a laminated structure in which the amount of particles of aeolian origin and their size create significant differences between the layers. This suggests inter-annual to inter-decadal variations in the strength of the local southerly winds responsible for (1) the erosion of the adjacent hyperarid surface of the Mejillones Pampa, and (2) the subsequent transport of the eroded particles towards the bay. A simple model accounting for the vertical uptake, transport, and deposition of the particles initially set into motion by wind at the surface of the pampa is proposed. This model, which could be adapted to other locations, assumes that the initial rate of (vertical) uptake is proportional to the (horizontal) saltation flux quantified by means of White's equation, that particles are lifted to a height (*H*), increasing with the magnitude of turbulence, and that sedimentation progressively removes the coarsest particles from the air column as it moves towards the bay. In this model, the proportionality constant (*A*) linking the vertical flux of particles with the horizontal flux, and the injection height (*H*) control the magnitude and size distribution of the deposition flux in the bay. Their values are determined using the wind speed measured over the pampa and the size distribution of particles collected in sediment traps deployed in the bay as constraints. After calibration, the model is used to assess the sensitivity of the deposition flux to the wind intensity variations. The possibility of performing such quantitative studies is necessary for interpreting precisely the variability of the aeolian material in the sediment cores collected at the bottom of Mejillones Bay. Copyright © 2010 John Wiley & Sons, Ltd.

KEYWORDS: wind erosion; sand transport modeling; deposition rate; Atacama Desert

Introduction

The coast of northern Chile provides a good illustration of the strength of the ocean/atmosphere/land interactions. In particular, the stress exerted on the ocean's surface by the coastal south/south-west winds, explains at the same time the cold northward Humboldt Current and the upwelling of nutrient-rich sub-surface water. Above a certain threshold depending on the surface characteristics, these winds can also set sand-sized particles into motion at the surface of unvegetated, or poorly-vegetated areas. Vargas *et al*. (2004, 2007) and Flores-Aqueveque *et al*. (2009, in Spanish but with an English abstract available online at *www.scielo.cl/andgeol.htm*; 2010) have shown that wind-erosion and the associated transport of particles along the direction of prevailing southerly winds not only explain some of the geomorphological features of Pampa Mejillones, a flat arid surface located south of the Mejillones Bay (Figure 1), but also the characteristics of the sediments collected in the bay at increasing distances from the shore. In particular, marine sediment cores collected 5 km downwind of the pampa present a layered structure in which the variability of the laminae has been associated by Vargas *et al*. (2007) with inter-annual to interdecadal variability in the strength of the southerly wind component.

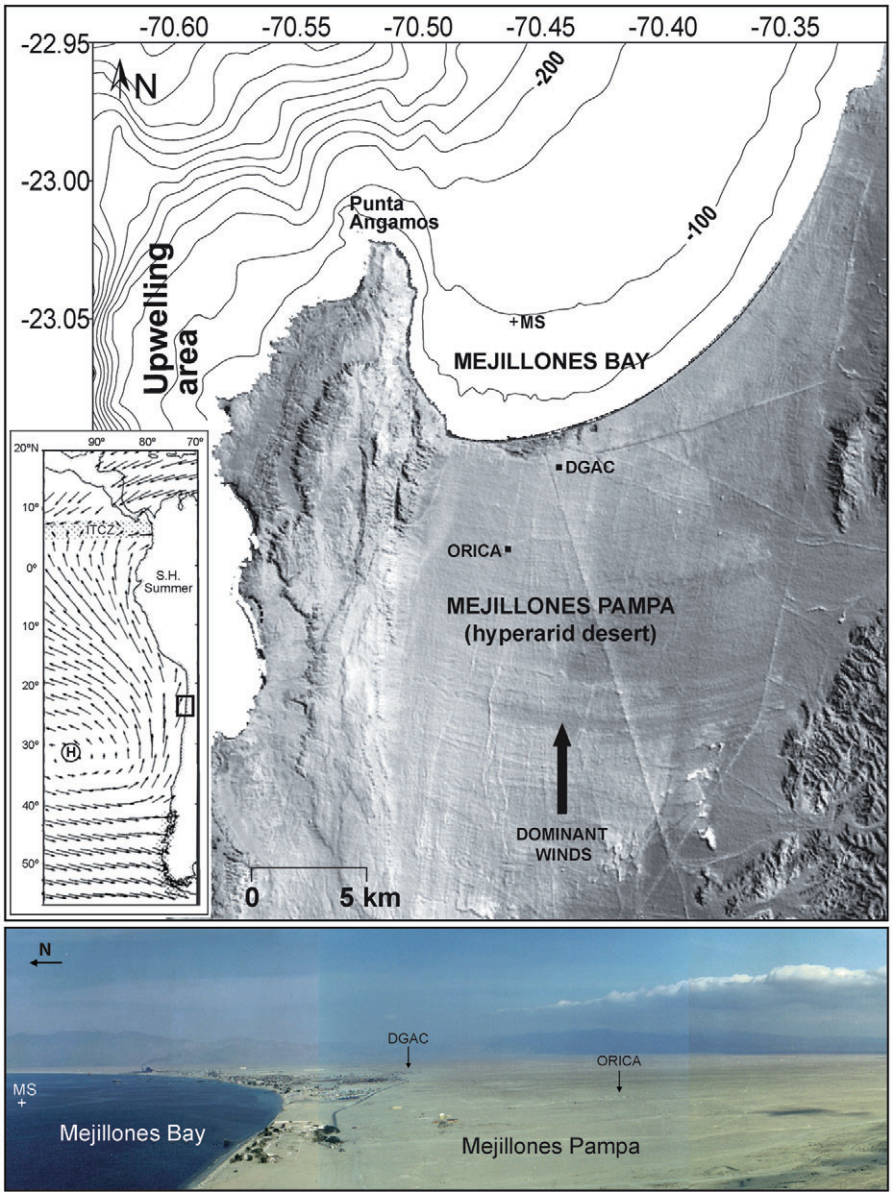

Figure 1. Map of the Mejillones Peninsula (23°S) with a schematic representation of the main local geomorphological features and the location of the ORICA and DGAC experimental stations. The position of the marine sampling site (MS) is also shown. This figure is available in colour online at wileyonlinelibrary.com/journal/espl

More generally, the information contained in marine sediments is invaluable for reconstructing present or past sedimentation-related processes. For instance, Stuut *et al*. (2007) used this information to assess the respective contributions of aeolian and fluvial sedimentation to the present day inputs of terrigenous material to the Chilean continental slope. By analyzing the terrigenous fraction of sediments recovered from Walvis Ridge in the SE Atlantic Ocean, Stuut *et al*. (2002) have been able to reconstruct the variability of the atmospheric circulation system over the last 300 kyr and to show that the Late Quaternary south-western African climate was relatively arid during the interglacial stages and relatively humid during the glacial stages. However, large uncertainties such as those related to the location and characteristics of the sources, to the particle transport paths and to deposition rates, can constitute an important obstacle to the accurate reconstruction of past aeolian fluxes in paleoenvironments.

The case of Mejillones Bay is better documented. Indeed, the terrestrial sediment source is well known since two field experiments (EOLOS 2006 and EOLOS 2008) have focused on the characteristics of the wind erosion flux at the pampa's surface (Flores-Aqueveque *et al*., 2009, 2010). In addition, during three periods, two of which coincided with EOLOS 2008, sediment traps were positioned in the water column to assess the magnitude and size distribution of the downward flux of aeolian mineral particles (Flores-Aqueveque *et al*., submitted). The closeness of the source and marine record facilitates the development of a model providing the missing quantitative link between the sediments that are blown at the surface of the pampa, transported offshore, and eventually recorded in the marine sediments. The interest in establishing a numerical relationship between the characteristics of the wind and those of the sediment layers (size distributions and abundance of lithic particles) is that it offers the possibility of reconstructing to some extent the variability of past winds over the period covered by the cores (*ca* 250 years BP; Vargas *et al*., 2004, 2007). Therefore, the present study focuses on the development of a simple model accounting for the transport and deposition of the mineral particles initially lifted from the surface of the pampa and subsequently moved towards the bay.

The first section of this paper summarizes the current state of understanding of the processes governing wind erosion at the surface of the pampa and presents the experimental data available for constraining the modeling of these emission/transport/deposition processes. The second part of the study details the physical principles on which the modeling is based. In the third part the model is calibrated using the results of the field

campaigns as constraints for evaluating the unknown parameters involved in the modeling. Finally, the calibrated model is used to assess the influence of wind strength on the magnitude and size distribution of the deposition flux at the surface of the bay.

Local Context and Summary of the Available Experimental Data

Sand movement at the surface of the pampa

Site description and soil characteristics

The Mejillones Peninsula, located in north Chile (23°S) corresponds to a physiographic feature whose geomorphology is dominated by a series of N–S oriented, uplifted and downfaulted blocks underlying an emerged coastal platform developed on marine sediments (Ferraris and Di Biase, 1978). Pampa Mejillones (Figure 1) is a flat surface of approximately 400 km^2 at the centre of this plain. Beach ridges of Pleistocene age (Ortlieb *et al*., 1996) and aeolian sand ripples (Flores-Aqueveque *et al*., 2010) can be observed over a large part of its surface (Figure 1).

Typically, the paleoridges are about 10 m wide, 2–5 m high, and in some cases more than 20 km long. They are made of coarse, fossiliferous, and poorly consolidated sediments. These ridges are particularly rich in large particles, mainly lithic fragments and pieces of shell with sizes up to 5 cm. The troughs between the crests contain particles of the same nature but of smaller size (<1 cm). At a depth of about 1 cm below the surface a salt and carbonated layer encrusting the sand-sized particles can be found. This light-coloured salt crust, which is only a few centimeters thick, could have been formed by the action of the pedogenetic processes prevailing in arid environments over the desiccated Pleistocene marine sediments. Below this layer, the sediments are very fine and well sorted.

In a recent work dedicated to the study of sand movements at the surface of Pampa Mejillones, Flores-Aqueveque *et al*. (2010) assessed the size distribution of soil samples collected in 17 different locations chosen for being representative of the variability of the surface state of the pampa. They found that the wind-erodible fraction of these soils (particles with diameter <840 μm) was always a mixture of at most three lognormally distributed populations of sand grains. The finest one (mode 1) has an approximate geometric mean diameter (gmd) of 130–140 μm and is observed in 13/17 cases. The second finest population (mode 2) is centered on a diameter between 200 and 300 μm and is even more common than mode 1. Indeed, it is observed in 15/17 cases. The coarsest population (mode 3) has a gmd between 400 and 600 μm and is present in 8/17 cases. These three modes of fine particles can easily be set into motion provided the stress exerted by the wind overcomes the forces (weight and inter-particle bonds) maintaining the sand grains on the soil's surface. This happens above a threshold wind friction velocity (u_t*) whose value depends on the surface roughness length (Z_0) (Alfaro and Gomes, 1995; Marticorena and Bergametti, 1995). Some geomorphologic features, such as the shape and orientation of aeolian ripples observed at the surface of the pampa, suggested that wind erosion events were mostly the result of strong winds blowing from the south, and therefore towards the bay. This was confirmed by the EOLOS 2006 and EOLOS 2008 field campaigns during which wind strength and direction were monitored along with the sand movement (Flores-Aqueveque *et al*., 2010) and whose results show that the erosion episodes are associated with the strengthening of the southerly winds during the afternoon.

Quantification of the sand movement

During the EOLOS campaigns, two different sites (Orica and DGAC, Figure 1) were equipped with masts, each supporting three traps of the Big Spring Number Eight (BSNE) type (Fryrear, 1986). These traps were positioned at heights ranging from 2 to 70 cm above the ground, which is inside the saltation layer, to catch the moving sand grains. The weighing of these particles allows quantification of the horizontal mass flux of particles (F_h), also referred to as the saltation flux. Flores-Aqueveque *et al*. (2010) showed that the measured saltation flux can be adequately simulated by the model of Marticorena and Bergametti (1995), or equivalently by White's (1986) equation, on which this model is based, provided the moderating effect of the paving of small stones present on the surface of the measurement site is accounted for. This is done by means of a proportionality constant K whose value is <1:

$$F_h = KF_{white} \tag{1}$$

where

$$F_{white} = \frac{\rho_a}{g} u^{*3}(1+R)(1-R^2) \tag{2}$$

In addition to the wind friction velocity (u*), this last equation also involves the air density (ρ_a = 1·23 kg m^{-3}), the gravitational acceleration (g = 9·81 m s^{-2}), and the ratio ($R = u_t^*/u^*$) of the saltation threshold to u*. Note that the horizontal flux is obtained in kg m^{-1} s^{-1} because it corresponds to the mass of particles crossing each second a vertical surface perpendicular to the wind direction, of unit width and infinite height.

The distribution of non-erodible small stones is not uniform at the surface of the pampa. Therefore, K, which represents the limiting effect of the stone paving on saltation, also depends on the location of the experimental site. More precisely, K was found to be close to 0·01 at Orica but three times larger at DGAC, where there was less gravel. Another, more indirect, effect of the non-erodible elements is that they increase the surface roughness and hence the threshold above which erosion is initiated. Although u_t* could not be determined exactly at DGAC where no meteorological measurements were made, the above-mentioned study of Flores-Aqueveque *et al*. (2010) showed that its value was lower than at Orica, where u_t* = 0·31 m s^{-1}.

The analysis of the size distribution of the material caught in the sand traps at different heights also revealed that the particles collected in the trap closest to the surface (less than 5 cm above it) mostly belonged to the two coarsest populations of wind erodible particles (modes 2 and 3). However, a relative enrichment in particles from mode 1 was observed in the highest traps (between 0·5 and 1 m above the surface). This increase with height of the proportion of particles with diameters around 100 μm was interpreted as resulting from the fact that they are more easily entrained by the upward component of turbulent air movements than the coarsest, and heaviest, particles. More generally, the vertical uptake of sand-sized particles is referred to as 'modified saltation' or equivalently 'short-term suspension' (Nalpanis, 1985; Gillette, 1979; Nishimura and Hunt, 2000). These relatively coarse particles simply extracted from the saltation flux must be distinguished from the much finer material released by the disaggregation (sandblasting) of the jumping sand grains when they hit the ground at the downwind end of their saltation trajectories. Indeed, sandblasting releases particles with sizes ranging typically from 0·1 to 20 μm (Alfaro and Gomes, 2001; Sow *et al*.,

Table I. Details of the three sampling periods (SPi) during which sediment traps were set up in Mejillones Bay. The geometric mean diameter (gmd, in µm), geometric standard deviation (gsd, dimensionless), and cumulated flux (flux, in mg m^{-2}) of the four populations (FSilt = Fine Silt, CSilt = Coarse silt, VFSand =Very fine sand, and FSand =Fine sand) of particles collected in the traps are also reported. Note that the FSand mode was detected only during one of the three sampling periods

	Sampling period			FSilt	CSilt	VFSand	FSand
Name	Beginning	End	Duration	gmd / gsd / flux	gmd / gsd / flux	gmd / gsd / flux	gmd / gsd / flux
SP1	05/01/2007	18/01/2007	13	12 / 2·2 / 1·7	38 / 1·3 / 0·7	83 / 1·3 / 0·7	–
SP2	25/09/2008	10/10/2008	16	15 / 2·2 / 1·6	37 / 1·4 / 1·0	84 / 1·4 / 6·6	–
SP3	10/10/2008	05/11/2008	25	13 / 2·2 / 2·9	41 / 1·4 / 3·5	80 / 1·3 / 8·6	125 / 1·2 / 8·3

2009), which is too small for them to be detected by the classical mass analysis methods applied to the sand-trap contents.

Characteristics of the deposition flux in the bay

In order to document the characteristics of the wind-transported mineral particles sedimenting in the bay, sediment traps were set-up on three occasions in the water column 5 km downwind (north) of the shore at two different depths. For the first sampling period the trap was located 15 m below sea surface (b.s.s.) whereas for the other two periods the traps were installed at 27 m b.s.s. The duration of the sampling periods varied between 13 and 25 days (see details in Table I). At the same time, meteorological measurements were performed on the pampa at the Orica experimental site. These measurements provide the 1 h averages of wind speed and direction at 4 m above ground level which will be necessary for the calibration of the particle uptake/transport/deposition model developed below.

A careful analysis of the mineral fraction of the traps' contents (Flores-Aqueveque *et al.*, submitted) showed that the deposition flux of wind-transported material is a mixture of four different populations with gmds ranging between approximately 10 and 120 µm. The details of these modes and the corresponding cumulated mass fluxes (in mg m^{-2}) for the three sampling periods are reported in Table I.

As discussed above, the finest particles constituting the FSilt mode could have been produced by sandblasting the sand grains moving on the surface of the pampa. Conversely, the other three modes are most probably due to the direct uptake, transport, and subsequent deposition of the populations of coarser particles originally present in the saltation flux. In the next section a physically-based model is proposed connecting explicitly the inputs of lithic material in the bay with the erosion at the surface of the pampa.

Designing the Uptake/Transport/Deposition Model

Assumptions

Along the south–north direction of the eroding winds the length (L) of the Pampa Mejillones is approximately 20 km (Figure 1). This fetch is discretized in a preset number (N) of equal sections. In this study N = 20, which means that the spatial step is 1 km, and each section will be referenced by means of an index i increasing from the southernmost position (i = 1) to the shore of the bay (i = 20) (Figure 2). Although we know that the flat surface of the pampa is not fully uniform, we will assume in our modelling that all its sections are equivalent. This homogeneity assumption implies that a unique set of parameters can be chosen for describing the sand movements over the whole extent of the source area. In particular, the values of K and u_t*, necessary for computation of the saltation flux according to Equation 1 and the roughness length (Z_0) necessary for the derivation of u* using the wind speed measurements at 4 m will be those determined for the Orica experimental site (0·01, 0·31 m s^{-1}, and 0·3 mm, respectively).

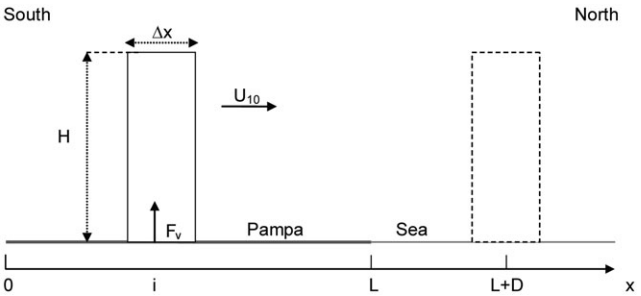

Figure 2. Scheme describing the geometry of the model. The length of the pampa (L = 20 km) along the prevailing direction of the eroding winds (south to north) is divided into 20 identical sections of length Δx = 1 km and referenced by their index (i). The marine deposition site is at a distance D (=5 km) north of the coast. For a given section, particles are injected into the air column of height H at a rate defined by the vertical upward flux F_v, which results in an initial concentration C_0 defined for each mode of particles. Owing to sedimentation during transport (at speed U_{10}), the air column is depleted of its coarser fraction on arriving at the marine deposition site (concentration C).

To represent the 'modified saltation' effect, which is to say the vertical uptake of a fraction of the saltating particles, we will consider that the uptake of each individual mode involved in the horizontal saltation flux is directly proportional to F_h. In other words, particles of these modes are injected from the surface into the air column (Figure 2) at a rate quantified by the following vertical injection flux:

$$F_{v,j} = A_j F_h \tag{3}$$

In this expression, the subscript j represents each of the sand-grain modes entering saltation and the A_j are unknown. Also note that the $F_{v,j}$ are in kg m^{-2} s^{-1}.

It also seems natural to consider that the stronger the turbulence (quantified by means of u^{*2}), the higher the particles will be lifted. Therefore the height (H) of the column into which they are injected should increase with u* above u_t*. We propose to consider here that this increase is scaled by the ratio $(u^*–u_t^*)^2$ g^{-1}, which has the dimension of a length, and that H is therefore given by:

$$H = \frac{\alpha}{g}(u^* - u_t^*)^2 \quad (4)$$

In this expression, α is an unknown dimensionless parameter. Note that for lack of experimental data we have considered that its value is independent of j, which means that particles of all sizes reach the same altitude in similar wind conditions.

Implications

Above any given section of the pampa, the initial columnar mass concentration ($C_{0,j}$) of particles from mode j resulting from an injection of duration Δt can be derived directly from Equations 3 and 4. Using also Equation 1, this yields:

$$C_{0,j} = \frac{gKA_j\Delta t}{\alpha(u^* - u_t^*)^2} F_{White} \quad (5)$$

Practically, the time step is fixed ($\Delta t = 1$ h), and u^* is derived from von Karman's equation describing the vertical profile of horizontal wind speed in neutral conditions:

$$u^* = kU_4/\ln(Z/Z_0) \quad (6)$$

In this equation k is von Karman's constant (=0·4), Z_0 has the value measured at Orica (=0·3 mm) and U_4 is the hourly-averaged wind speed measured at height Z (=4 m). Note that although maximum particle-eroding wind speeds occur in connection with high insolation over the pampa, high winds speeds secure near neutral wind profiles within the first 10 m above the ground.

Based on the observation that the size distribution of the saltating particles caught in the BSNE traps is a combination of log-normal modes, we will also consider that the initial distribution of the uplifted particles, and hence of $C_{0,j}$, is well described by this model:

$$\frac{dC_{0,j}}{d\ln d} = \frac{C_{0,j}}{\sqrt{2\pi}\ln\sigma_g}\exp\left[-\frac{(\ln d - \ln d_g)^2}{2(\ln\sigma_g)^2}\right] \quad (7)$$

in which d_g is the geometric mean diameter (gmd), σ_g the geometric standard deviation (gsd), and $C_{0,j}$ the amplitude characterizing this initial distribution.

The content of the column initially located above the ith section of the pampa is not stationary. It moves towards the north at a speed that can be scaled by the average wind speed at an arbitrary reference height, for instance the one (10 m) classically used in meteorological measurements. In our experiments, this wind speed (U_{10}) can be derived using Equation 6 and the speed measured onsite at 4 m (U_4). In the dry context of the Atacama Desert, dry deposition is the only process responsible for the removal of air suspended particles during transport. For particles with sizes much above 1 µm, which is the case of those concerned with modified saltation, Brownian diffusion and impaction can be neglected and deposition is controlled by gravitational settling (Seinfeld and Pandis, 1998). Because according to Stokes-Einstein's law the settling velocity (V_{sed}) increases with size, the largest particles are removed (fall) more rapidly than the fine ones and the initial content of the air column is progressively depleted of its coarsest fraction. For details of the computation of V_{sed}, we refer the reader to Foret *et al*. (2006).

In the moving column, the rate of removal of a given size class is given by the deposition flux, which is to say the product of the current concentration and V_{sed}. This leads to an exponential decrease with time of the concentration described by:

$$\left[\frac{dC_j}{d\ln d}\right](t) = \left[\frac{dC_{0,j}}{d\ln d}\right]\exp\left(-\frac{V_{sed}}{H}t\right) \quad (8)$$

Keeping in mind that we want to quantify the size-resolved mass of particles transported to the point where the sediment traps were implemented in the bay, which is to say at a fixed distance (D = 5 km) downwind of the coastline, t must be replaced in Equation (8) by the time (τ_i) it takes the particles to go from the ith section of the source area to this particular location. At the speed U_{10}, and taking into account that L, D, and i are initially expressed in kilometers, this time is:

$$\tau_i = 1000(L + D - i)/U_{10} \quad (9)$$

Finally, considering that the global concentration above the sea is the sum of the individual contributions of the N sections of the pampa, and multiplying by the sedimentation velocity, one obtains the size-resolved deposition flux for mode j as:

$$\left[\frac{dF_{dep,j}}{d\ln d}\right] = \left[\frac{dC_{0,j}}{d\ln d}\right]V_{sed}\left[\sum_{i=1}^{N=20}\exp\left(-\frac{gV_{sed}}{\alpha(u^* - u_t^*)^2}\tau_i\right)\right] \quad (10)$$

The total mass flux of mode-j particles deposited at the sea surface is obtained by a simple summation of Equation 10 over the size classes. Also note that this flux is the one corresponding to particles initially emitted during a unique time step Δt (1 h in our study), and that for longer emissions such as those corresponding to the sampling periods of the marine sediment traps, integration over time is also necessary.

Model Calibration and Sensitivity Study

Methodology

Several parameters are involved in the equations of the model. Some of them, such as K, Z_0, and u_t^*, have been determined experimentally for at least one site (Orica). Because the stone paving at this site tends to be more developed than elsewhere, these experimental values might constitute a slight overestimation for the rest of the pampa. Nevertheless, comparison of the erosion flux at Orica with the one measured at DGAC suggests that at least their orders of magnitude are representative of the pampa surface conditions and we will use these values in the rest of the computations. The uncertainty in the parameter (α) scaling the initial injection height (H) of the particles is large. A first guess is that in medium to strong erosion conditions the uplifted particles reach altitudes that compare with the typical height of the mixing layer, which is to say at least a few hundred meters (Stull, 1988). Equation (4) shows that for u^* varying between u_t^* and 0·6 m s^{-1} (approximately twice the saltation threshold) such altitudes are obtained for α values between 10^4 and 10^6. We detail below how a more precise value of α can be assessed.

Contrary to the other parameters for which at least an order of magnitude was available through measurements or could be

estimated, the A_j are completely unknown. Indeed, to the best of our knowledge there exists no information in the literature on the rate at which 'giant' particles are extracted from the saltation flux and entrained into 'modified saltation'. It is also the objective of the following calibration to determine the A_j values for the area of study. The principle of this calibration is as follows: the model can be run for each soil mode using the wind data collected during the three periods of the marine traps sampling.

In the first phase of the calibration we seek the order of magnitude of α. For this the A_j are initially set equal to 1 and we use the fact that through its influence on H, α not only conditions the initial particle concentration in the air column but also the rate at which the coarsest particles are removed from it during transport. This implies that the smaller α is, the larger the shift towards small diameters of the size distribution observed at the marine site. Practically, the α value will be determined as the one yielding the best agreement between the modeled and the measured size distributions of the deposited particles.

The second phase of the calibration consists in determining the A_j. These parameters will be obtained by fitting the cumulated mass flux of each transported soil mode calculated with the model to those measured with the sediment traps during the three measurement periods.

Results

Erosion conditions on the pampa and consequences for the marine deposition flux

During the first two periods of marine sampling (SP1 and SP2) the hourly-averaged u^* on the Pampa became larger than the saltation threshold on 80 and 63 occasions, respectively. This occurred 143 times during the third sampling period (SP3), this larger number being probably due in part to the fact that SP3 lasted longer than the other two periods. Calculated using Equations (1) and (2) and the hourly u^* values, the horizontal saltation flux cumulated over the durations of the three periods was 8·3, 10·2, and 19·2 kg m^{-1} for SP1, SP2, and SP3, respectively. A statistical analysis of the distributions of the hourly values of this flux (Figure 3) shows that these distributions are approximately bi-modal in the three cases. The first mode in the distribution is centered on a wind friction velocity between 0·36 and 0·38 m s^{-1} whereas the second mode is centered on a value between 0·44 and 0·48 m s^{-1}. During SP2 the number of eroding hours corresponding to the largest mode ($u^* >$ 0·42 m s^{-1}) was approximately the same as during SP3 (16 and 17, respectively), but such large u^* values were achieved only 10 times during SP1. This lower number of occurrences of strong eroding winds during SP1 could explain the fact that the deposition flux in the bay in this period is less rich in coarse particles than during SP2 and SP3. Indeed, Figure 4 shows that the ratio of the deposition fluxes measured in the marine traps during SP2 and SP1 is close to 1 for particles with diameters <40 μm, but increases sharply above this value. This suggests that the uptake or/and transport of medium sized particles could be less efficient during SP1 than during the other two periods. Conversely, comparison of the fluxes measured during SP3 and SP2 reveals that their size distributions are similar. These two fluxes only differ in amplitude, the one during SP3 being almost uniformly twice the one of SP2 in the whole 10–100 μm size range.

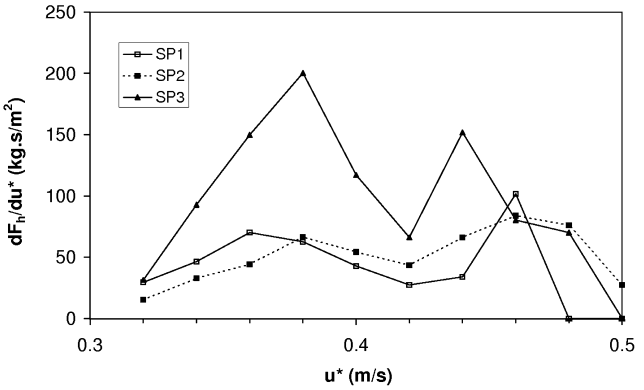

Figure 3. Statistical distribution of the hourly horizontal flux (dF_h/du^*) at the surface of the pampa for the three periods (SP_i) of the marine trap sampling.

Calibration of the injection height (α)

In order to test the sensitivity of the deposition flux size distribution to α, the model has been used to simulate the transport and deposition of the mode of soil particles centered on 130–140 μm (mode 1) during the longest observation period (SP3). For the computations, the value of the unknown proportionality constant A_1 has been provisionally fixed at 1 and several values of α selected between 10^4 and 10^6. As expected, Figure 5 shows that the transport of particles smaller than approximately 40 μm is relatively insensitive to changes in α. Conversely, more particles of increasingly large diameters are able to reach the deposition site as their initial injection height

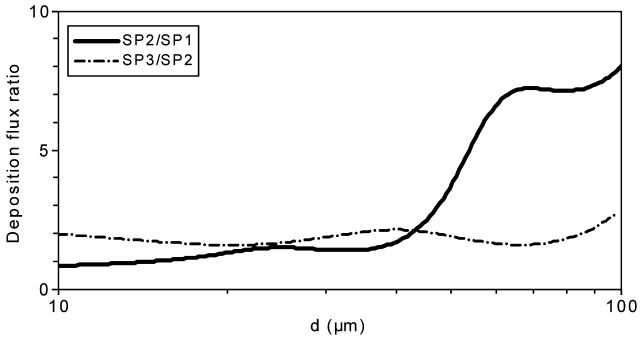

Figure 4. Comparison of the size distributions of the deposition fluxes of aeolian particles collected in the marine sediment traps for three different sampling periods (SP1, SP2, and SP3).

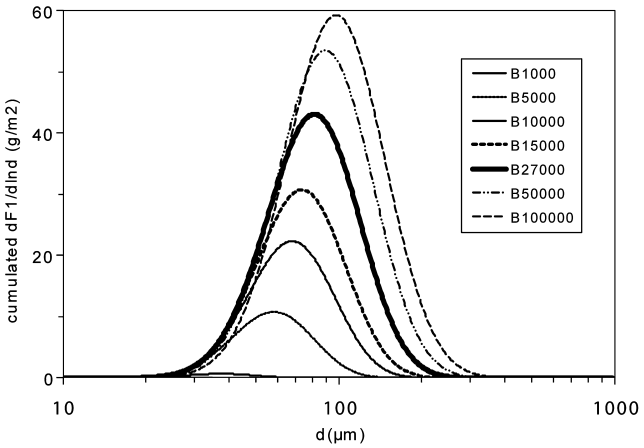

Figure 5. Influence of the injection height parameter (α) on the deposition flux of particles from the M mode in Mejillones Bay. Note that the values of α used for the runs and reported in the box have been divided by 1000 (e.g. 10 should be read 10,000).

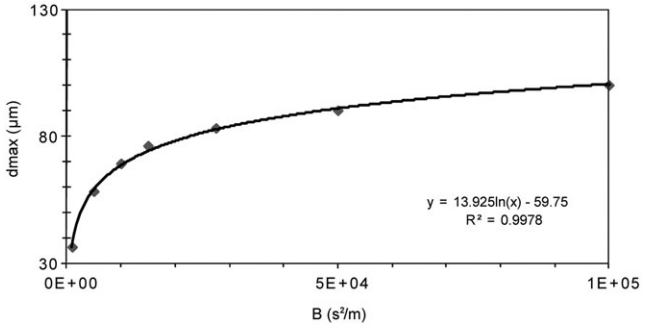

Figure 6. Impact of the injection height parameter (α) on the size of the particles deposited in the bay (see text for details).

(or α) over the pampa increases. As a consequence, the diameter (d_{max}) for which the maximum value of the deposition flux is obtained also increases with α. Note that due to the selective deposition of the coarsest particles during transport, the size distribution of the deposition flux is shifted towards small sizes compared with the distribution of the original soil mode. In particular, the fact that the $d_{ma.x}$ observed on Figure 5 are in the same range of values as the gmd (~80 µm) of the VFSand mode collected in the marine traps (see Table I) suggests that this VFSand mode could be the direct result of the transport of soil mode1. Numerically, the dependence of d_{max} on α is found to be represented perfectly (r^2 = 0·998, see Figure 6) by the following equation:

$$d_{max} = 13{\cdot}9\ln(\alpha) - 91{\cdot}4 \quad (11)$$

Equation 11 allows determination of the order of magnitude of α using the values of d_{max} (from 80 to 84 µm) measured during the three sampling periods. The value ($\alpha = 270 \times 10^3$) obtained by this method will be retained for future computations. In particular the transport of the coarsest soil mode (mode 2) can be simulated with it. The size shift due to the rapid fall during transport of these very coarse particles is even more important than for mode 1. For instance, in the case of SP3 the model yields a d_{max} value of 135 µm at the deposition site, which is much less than the initial gmd (=210 µm) of mode 2. Also interesting is that this calculated d_{max} is close to the gmd (125 µm, see Table I) of the fine sand (FSand) mode determined experimentally in the size analysis of the content of the marine sediment traps. This indicates that exactly as the VFSand mode of the deposition flux could be linked to soil mode 1, the FSand mode is probably due to the transport of at least the finest fraction of soil mode 2. In a similar manner, the presence of the fine silt (FSilt) mode has been interpreted previously as being the result of the transport and deposition of particles initially produced by sandblasting of the sand grains saltating at the surface of the pampa. The origin of the coarse silt (CSilt) mode appearing in Table I is less clear. These fine particles could either have been present as such in the original soil or have been produced by a breaking process similar to sandblasting. In any case, like the FSilt mode, these particles were not detected in the mass analysis of the contents of the BSNE sand traps implemented at the surface of the pampa. The reason for this is probably that, due to their relatively small size, the mass they represent is much smaller than that of the coarser soil modes. Because the particles of the fine silt mode have diameters <40 µm, which is to say in the range where the shift in size predicted by the model is relatively small (see above), we will assume that the gmd and geometric standard deviation (gsd) of their 'father' mode (hereinafter referred to as mode 0) on the pampa are the same (35 µm and 1·4) as those at the deposition end of its trajectory.

In summary, besides the mode of particles produced by sandblasting and eventually deposited in the bay in the form of the fine silt mode, there are three other soil modes (modes 0, 1, and 2) whose rate of injection into the air column must be calibrated.

Calibration of the uptake of coarse particles by modified saltation (A_j)

As recalled above, the two populations of relatively fine sand grains (modes 1 and 2) identified in almost all the 17 soil samples collected at the surface of the pampa and detected in the moving material collected close to the surface of the source are at the origin of the VFSand and FSand modes found in the marine samples. The coarsest wind-erodible soil mode (mode 3), which was also observed in half of these soil samples, does not seem to contribute significantly to the deposition flux. Indeed, only very few particles with diameters >100 µm, and none with d > 150 µm were collected in the deposition traps. This suggests that, at least in the conditions prevailing during the three measurement periods, wind never became strong enough to transport the coarsest particles of mode 3 to the marine sampling site. The number of particles of the FSand mode collected in the traps was also quite reduced. For instance Flores-Aqueveque *et al*. (submitted) indicate that only 14 particles larger than 100 µm were collected in the marine traps during SP3 and even less during the shorter durations of SP1 and SP2. Our calibration efforts will bear first on mode 0 and mode 1, which were found in larger quantities in the traps. Because it is similar to the one for mode 0, the case of the FSilt mode of sandblasted particles will then be discussed. Finally, the uptake of mode 2 will be treated. In this last case, the precision is expected to be less than in the other cases because the FSand mode was detected during only one sampling period (SP3).

In the modeling, the initial gmd and gsd values of mode 1 (100 µm and 1·6) are those determined in the size analysis of the highest BSNE trap whose content was the richest in this mode. For similar reasons, the values retained for mode 2 (210 µm and 1·5) are those obtained at the lowest level. Finally, it has been indicated above how the values for mode 0 (35 µm, 1·4) can be deduced from observation of the marine sediments.

When calculated with A_0 = 1 the flux of mode 0 particles deposited at the location of the sediment traps during a measurement period is a gross overestimation of the measured cumulated flux of the CSilt mode. The best fit between measurements and model outputs is obtained for $A_0 = 5{\cdot}4 \times 10^{-8}$ m^{-1}. As illustrated on Figure 7(a), the cumulated deposition flux is directly proportional to the cumulated saltation flux ($F_{h,cum}$) on the pampa. This suggests that, at least for this mode, the effect of transport is not different in the three sampling periods, meaning in turn that the main factor controlling the arrival of CSilt particles at the sea site is the rate at which they were initially uplifted on the pampa, this rate itself directly proportional to F_h as assumed in the development of the model. Also interesting is that the correlation between the deposition flux and $F_{h,cum}$ is the same for the CSilt mode and the FSilt mode produced by sandblasting (Figure 7(a)). Although the sandblasting process is known to be physically much more complicated than a simple uplift of particles (Alfaro *et al*., 1997), we will simplify the modeling of the uptake, transport and deposition of the sandblasted particles by considering that these processes can be modeled like those of the coarser particles entrained by modified saltation. Because many experimental studies have demonstrated that

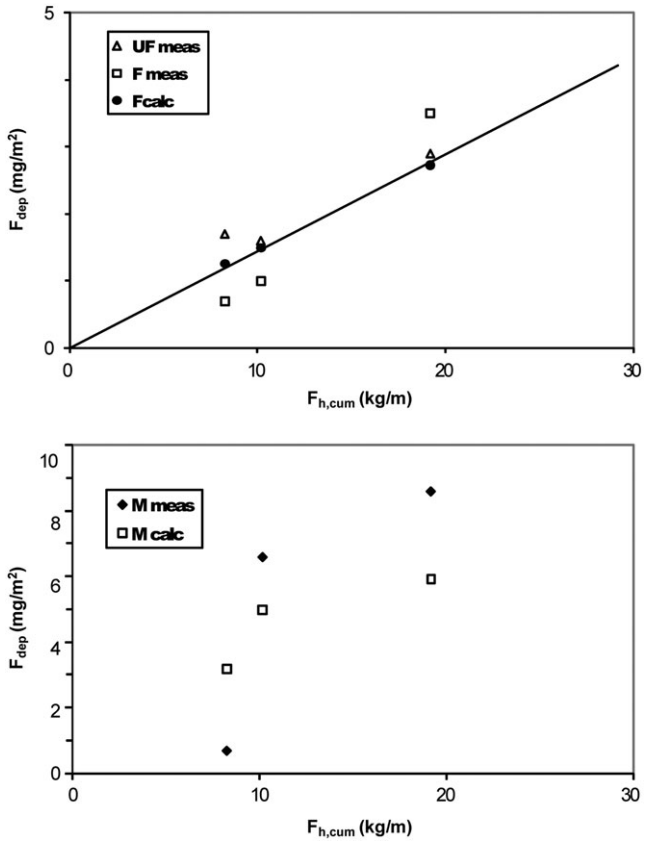

Figure 7. Correlation of the cumulated mass deposition flux (F_{dep}) of particles with the cumulated erosion flux ($F_{h,cum}$) on the pampa for the three sampling periods: (a) cases of the very fine (VFSilt) and fine (FSilt) silt modes, and (b) the VFSand mode. The prediction of the model is also shown for the FSilt mode (straight line).

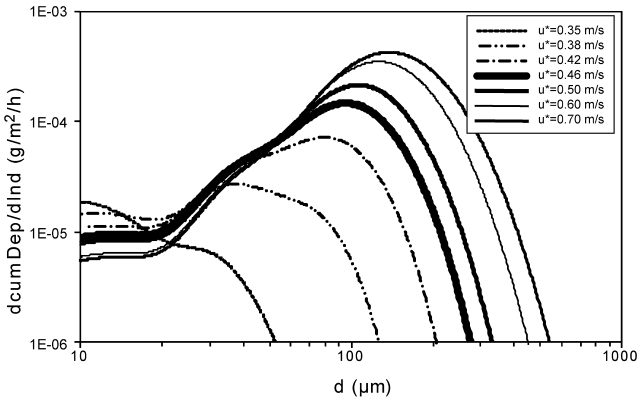

Figure 8. Size distributions of the deposition flux predicted by the model at increasing u^*.

the sandblasting process releases particles with sizes mostly between 1 and 10 µm, the initial size distribution of these particles will be assumed to be monomodal, centered on 5 µm, and with a gsd (=2·0) large enough to encompass this size range. With these input data, the modeled deposition flux of sandblasted particles is found to be in the best possible agreement with the measured one when A_{sand} = 1·39 × 10^{-7} m^{-1}. This last parameter is in fact similar to the sandblasting efficiency defined by Gillette (1977) as the ratio of the vertical flux of very fine (<20 µm) particles released by the impacts of saltating sand grains to the horizontal saltation flux. Field measurements of this efficiency have shown (Gillette, 1977; Nickling and Gillies, 1989; Gomes *et al.*, 2003; Alfaro *et al.*, 2004) that its value generally varies between 10^{-6} and 10^{-4} m^{-1}. Note that our value of A_{sand} is sensitive to a possible underestimation (or overestimation) of the saltation flux, resulting itself from an overestimation (underestimation) of the soil roughness length when using the Orica value for the whole surface of the pampa. However, regarding this point it may be noted that the quantity defining the initial particle concentration in the air column (Equation 5) is the product of K and A_j. Therefore, although leading to an overestimation of A_j, the possible underestimation of K does not affect the product of the two quantities and the final characteristics of the deposition flux based on Equation 5 are not biased significantly by the initial error on K.

The same calibration procedure applied to soil mode 1 reveals that for sizes coarser than those of the FSilt and CSilt modes, the cumulated deposition flux is not simply proportional to $F_{h,cum}$ (Figure 7(b)). This reflects the complex influence on transport of the statistical distribution of the wind speed values above the saltation threshold and their difference of patterns during the three sampling periods. The sensitivity of the deposition flux to the individual hourly values of u^* and to their combination during long observation periods will be further discussed below after the calibration. The best fit (Figure 7(b)) between the modelled and measured deposition fluxes of the VFSand mode is obtained for A_1 = 1·43 × 10^{-7} m^{-1}.

As already discussed above, the only deposition flux data available for the determination of A_2 are those of SP3. Indeed, the magnitude of the flux of FSand particles could not be assessed during SP1 and SP2 because only four or five lithic particles with diameters >100 µm were observed in the corresponding marine samples. Due to the longer duration of the sampling, 14 such particles were caught in the marine trap deployed during SP3, which was enough to require the use of the FSand mode in the fitting of the measured size distribution. Finally, A_2 (=7·90 × 10^{-7} m^{-1}) is simply the ratio of the measured cumulated flux of these particles to the one computed with the model.

The determination of A_j and α have completed the model, which can be used to quantify the impact of the meteorological conditions prevailing at the surface of the pampa on the characteristics of the deposition flux at the marine site.

Sensitivity of the deposition flux to wind speed

For calibration of the model we have relied on experimental data collected during sampling periods which lasted from 13 to 25 days. By the simple effect of averaging, integration over such long durations of the model's outputs tends to blur the real individual impact of the key input parameters of the model. This is particularly the case for wind speed, whose intensity varies at high frequency over the surface of the pampa. In order to check the effect of wind on the characteristics of the deposition flux at the location of the marine traps, we have used the calibrated model to compute the size-resolved cumulated mass flux produced by events of fixed duration (1 h) and of increasing intensities. The results (Figure 8) show that for diameters <20 µm the deposition flux is not very sensitive to wind speed, which explains the fact that the deposition fluxes do not differ by more than a factor 2 between the three sampling periods.

Conversely, the proportion of medium-size and giant particles increases rapidly with u^*.

Note that the overall mass deposition flux is very sensitive to this change in size distribution and that the intensity of the flux increases sharply with u^* above the saltation threshold

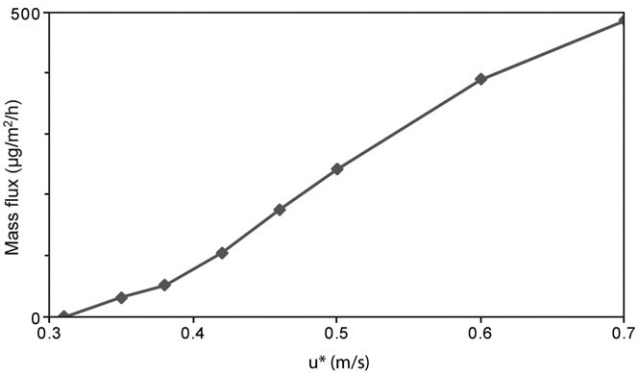

Figure 9. Influence of u^* on the intensity of the mass deposition flux at the location of the marine traps in Mejillones Bay.

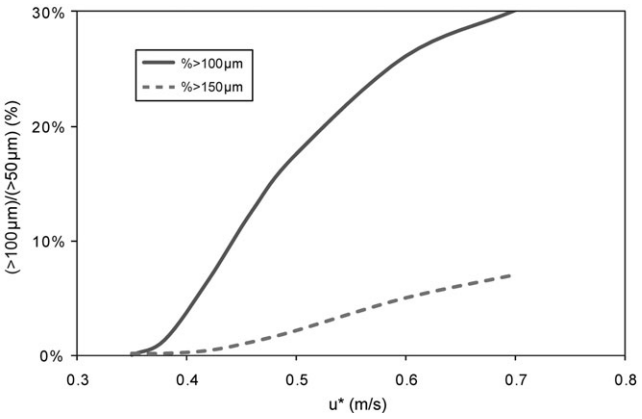

Figure 10. Influence of the wind friction velocity on the proportion of particles coarser than 100 and 150 µm in the deposition flux relative to those with diameters >50 µm.

(Figure 9). Coming back to the size-resolved flux, Figure 8 also shows that the observation of very coarse particles requires that u^* has reached a certain value. For instance, the model predicts that particles coarser than 100 µm only appear in the deposition flux for $u^* > 0{\cdot}38$ m s^{-1}.

The size-resolved number deposition flux (in particles m^{-2} h^{-1}), which can easily be derived from the mass flux assuming that the particle are spherical and have the same density as quartz (2·65 g cm^{-3}) is also useful. Indeed, this flux allows prediction of the number of particles of a given size expected to be caught in a sediment trap of fixed opening in given wind conditions. It also allows computation of the proportion of particles larger than a given size in the overall, or in a fraction of, the deposition flux. For instance Figure 10 displays the percentage of particles larger than 100 µm in the flux of particles with diameters >50 µm. This percentage is found to increase from 0 (at $u^* = 0{\cdot}35$ m s^{-1}) to 30% (at 0·70 m s^{-1}), whereas the fraction of particles larger than 150 µm is 0 for $u^* < 0{\cdot}42$ m s^{-1} and remains no larger than 2% up to the relatively large friction velocity of 0·5 m s^{-1}. Retrospectively, the fact that this u^* value was never reached during the three sampling periods explains why particles with diameters >150 µm were not detected in the analysis of the contents of the sediment traps. In any case, the possibility of correlating precisely the magnitude of the deposition flux and its size-characteristics with the strength of the wind on the pampa is a precious tool for understanding the variability of the aeolian component in the sediment core collected at the bottom of Mejillones Bay.

Summary and Conclusion

In this work we have developed a simple but physically explicit model for linking the characteristics of the deposition flux of aeolian particles inside Mejillones Bay, with the strength of the dominant southerly winds. Note that although initially developed in a local context, the proposed methodology could be adapted to other locations. The model is based on the assumption that the sand grains moved by wind at the surface of the pampa can be entrained upwards by turbulence (the so-called 'modified saltation' process). The initial particle concentration in the air column above a given section of the source increases with the efficiency of this uptake, assumed to be simply proportional to the intensity of the saltation flux, but decreases with the height of injection (H), the latter depending on the intensity of the turbulence. Because the higher coarse particles are initially raised above the pampa, the farther they can be transported before falling into the sea, H also conditions in great part the magnitude of the shift in size distribution between the source and the marine deposition site. Practically, we have used the measured size distribution of the deposition flux for determining the constant (α) involved in the parameterization of H. In a second phase the intensity of the deposition flux measured for each particle mode has been used as a constraint for determining the rate of vertical uptake of the particles saltating at the surface of the source. The fact that the calibrated model allows retrieval of the characteristics (intensity and size distribution) of the deposition flux validates the assumptions on which it was initially based. Therefore the model can be used to make numerical predictions of these characteristics. In particular, the influence of the wind speed near the surface of the source can be assessed, which was not possible with the results of the long integration periods of the marine traps sampling. This possibility of correlating precisely the amount and size distribution of the flux of particles deposited at the surface of the sea with local meteorological conditions was a prerequisite for interpreting the variability of the aeolian material contained in the sediment cores collected at the bottom of Mejillones Bay. More generally, the fine time resolution (1 h) of the proposed model is well adapted to the short time-scales of the emission of mineral particles by wind erosion. Therefore, this methodology could prove useful in any study trying to interpret precisely the variability of the aeolian content of marine sediments.

Acknowledgments—This work was carried out within the framework of an international scientific collaboration between the University of Chile (Department of Geology and Department of Geophysics), the University of Antofagasta (Faremar), the University of Paris XII (LISA), and the IRD (LOCEAN), supported by the ECOS-CONICYT #C05U03 cooperation project. Field experiment and data acquisition were funded by project Fondecyt 11060484 and PRODAC, University of Chile.

References

Alfaro SC, Gomes L. 1995. Improving the large-scale modelling of the saltation flux of soil particles in presence of non-erodible elements. *Journal of Geophysical Research* **100**: 16357–16366.

Alfaro SC, Gomes L. 2001. Modeling mineral aerosol production by wind erosion: emission intensities and aerosol distributions in source areas. *Journal of Geophysical Research* **106**: 18075–18084.

Alfaro SC, Gaudichet A, Gomes L, Maillé M. 1997. Modelling the size distribution of a soil aerosol produced by sandblasting. *Journal of Geophysical Research* **102**: 11239–11249.

Alfaro SC, Rajot JL, Nickling W. 2004. Estimation of PM20 emissions by wind erosion: main sources of uncertainties. *Geomorphology* **59**: 63–74.

Ferraris F, Di Biase F. 1978. *Hoja Antofagasta, región Antofagasta*. Carta Geologicas, Chile no 30, Instituto de Investigaciones Geológicas Chile, 1 map 1:250.000.

Flores-Aqueveque V, Vargas G, Rutllant J, Le Roux JP. 2009. Parametrización, estacionalidad y sedimentología del transporte eólico de partículas en el desierto costero de Atacama, Chile (23°S). *Andean Geology* **36**(2): 288–310.

Flores-Aqueveque V, Alfaro SC, Muñoz R, Rutllant J, Caquineau S, LeRoux J, Vargas G. 2010. Aeolian sand transport over the Pampa Mejillones in the coastal Atacama Desert of northern Chile. *Geomorphology* **120**(3–4): 312–325.

Flores-Aqueveque V, Caquineau S, Alfaro S, Valdés J, Vargas G. Using image-based size-analysis for assessing the size distribution of aeolian particles sampled in a coastal upwelling system off northern Chile (23°S). Submitted to *Estuarine, Coastal and Shelf Science*.

Foret G, Bergametti G, Dulac F, Menut L. 2006. An optimized particle size bin scheme for modelling mineral dust aerosol. *Journal of Geophysical Research* **111**: D17310. doi:10.1029/2005JD006797.

Fryrear DW. 1986. A field dust sampler. *Journal of Soil and Water Conservation* **41**(2): 117–120.

Gillette DA. 1977. Fine particulate emissions due to wind erosion. *Transactions of the American Society of Agricultural Engineers* **20**(5): 890–897.

Gillette DA. 1979. Environmental factors affecting dust emissions by wind erosion. In *Saharan Dust*, Morales C (ed). Wiley: New York; 71–94.

Gomes L, Rajot JL, Alfaro SC, Gaudichet A. 2003. Validation of a dust production model from measurements performed in semi-arid agricultural areas of Spain and Niger. *Catena* **52**: 257–271.

Marticorena B, Bergametti G. 1995. Modeling the atmospheric dust cycle. *Journal of Geophysical Research* **100**: 16415–16430.

Nalpanis P. 1985. Saltating and suspended particles over flat and sloping surfaces. II. Experiments and numerical simulations. In *Proceedings of the International Workshop on the Physics of Blown Sand*, Barndor-Nielsen OE (ed). vol. **1**, 37–66. Mem. 8, University of Aarhus: Denmark.

Nickling WG, Gillies JA. 1989. Emission of fine-grained particulates from desert soils. In *Paleoclimatology and Paleometeorology: Modern and Past Patterns of Global Atmospheric Transport*, Leinen M, Sarntheim M (eds). Kluwer Academic Publishing: Dordrecht; 133–165.

Nishimura K, Hunt JCR. 2000. Saltation and incipient suspension above a flat particle bed below a turbulent boundary layer. *Journal of Fluid Mechanics* **417**: 77–102.

Ortlieb L, Díaz A, Guzmán N. 1996. A warm interglacial episode during Oxigen Isotope Stage 11 in northern Chile. *Quaternary Science Reviews* **15**: 857–871.

Seinfeld JH, Pandis SN. 1998. *Atmospheric Chemistry and Physics: from Air Pollution to Climate Change*. John Wiley: New York.

Sow M, Alfaro SC, Marticorena B, Rajot JL. 2009. Size resolved dust emission fluxes measured in Niger during 3 dust storms of the AMMA experiment. *Atmospheric Chemistry and Physics* **9**: 3881–3891.

Stull RB. 1988. *An Introduction to Boundary Layer Meteorology*. Kluwer Academic Publishers: Dordrecht.

Stuut JBW, Prins MA, Schneider RR, Weltje GJ, Jansen JHF, Postma G. 2002. A 300-kyr record of aridity and wind strength in southwestern Africa: inferences from grain-size distributions of sediments on Walvis Ridge, SE Atlantic. *Marine Geology* **180**(1-4): 221–233, doi:10.1016/S0025-3227(01)00215-8.

Stuut JBW, Kasten S, Lamy F, Hebbeln D. 2007. Sources and modes of terrigenous sediment input to the Chilean continental slope. *Quaternary International* **161**(1): 67–76. doi:10.1016/j.quaint.2006.10.041.

Vargas G, Ortlieb L, Pichon JJ, Bertaux J, Pujos M. 2004. Sedimentary facies and high resolution primary production inferences from laminated diatomaceous sediments off northern Chile (23°S). *Marine Geology* **211**: 79–99.

Vargas G, Pantoja S, Rutllant J, Lange C. Ortlieb, L. 2007. Enhancement of coastal upwelling and interdecadal ENSO-like variability in the Peru-Chile current since late 19th century. *Geophysical Research Letters* **34**: L13607, doi: 10.1029/2006 GL0288127.

White BR. 1986. *Encyclopedia of Fluid Mechanics*. Gulf: Houston, TX; 239–282.

